JACS
JOURNAL OF THE AMERICAN CHEMICAL SOCIETY
pubs.acs.org/JACS
Communication

The Role of Protons in CO_2 Reduction on Gold under Acidic Conditions

Weixing Wu and Ying Wang*

Cite This: J. Am. Chem. Soc. 2025, 147, 11662−11666
Read Online
ACCESS | Metrics & More | Article Recommendations | Supporting Information

ABSTRACT: Carbonate formation constitutes a major obstacle in the electrochemical CO_2 reduction reaction (CO_2RR), restricting the industrial implementation of this reaction. Even when adopting mild acidic electrolytes, carbonate formation is still observed. The fundamental reason lies in the inevitable OH^- generation when H_2O is the proton donor, leading to subsequent carbonate formation. Thus, exploring the reaction pathway of the CO_2RR in the acid, especially if a proton can directly participate in the reaction, is critical. Herein, we employed a rotating ring-disk electrode and surface interrogation scanning electrochemical microscopy to investigate the electrode process of the CO_2RR in acid. A pH-dependent behavior of CO_2RR is observed, indicating proton acting as the reactant in the RDS, originating from the early onset of CO_2 adsorption under locally acidic conditions.

Electrochemical CO_2 reduction reaction (CO_2RR) driven by renewable electricity is an attractive approach to achieve decarbonization for chemical/fuel production.[1−3] Substantial progress has been made in advancing this reaction to industrial-relevant conditions, i.e., high current density and high selectivity, yet the challenge ahead is to resolve the well-known "carbonate issue".[4,5] The inevitable reaction between alkaline/neutral electrolyte and CO_2 feed consumes a major amount of reactant to produce (bi)carbonate, rendering a frustrating CO_2 utilization and poor device stability.[6] Acidic media is employed to avoid (bi)carbonate formation, which can achieve a high single-pass carbon utilization efficiency—up to 90% for CO production,[7] 85% for C_{2+},[8] exceeding the theoretical limit in the neutral case.[6] However, the formation of carbonate is still observed at long-term electrolysis in the most used mildly acidic conditions, causing stability issues at the device level.[6,9−11]

The carbonate issue in acidic media originates from (1) the difference of charge transfer rate versus mass transport and (2) the chemical identity of the proton donor. For example, four electrode reactions can occur for CO production (eqs 1−4). If eqs 1 and 2 dominate, a rapid mass transport rate is required to counterbalance OH^- generation as H_2O is the proton donor.[12,13] However, the charge transfer rate increases exponentially with applied potential, as described by the Buter−Volmer equation,[14] while the mass transport rate is independent (Scheme S1a). If taking 500 mA/cm^2, the current density for a mature water electrolyzer, the production rate of OH^- is 5 μmol cm^{-2} s^{-1}, a few magnitudes larger than the proton transport rate considering typical pH = 2 electrolyte and 100 um diffusion layer thickness (2×10^{-2} μmol cm^{-2} s^{-1}). Only when an acidic local environment is maintained by using strongly acidic electrolyte (e.g., pH = 0), carbonate formation can be eliminated (Scheme S1b). In this case, proton reduction (eq 4) will be dominant if water is the only viable proton source for the CO_2RR (eq 1) due to the distinct kinetic. Thus, a critical knowledge gap lies in finding out if H^+ can act as the proton donor for CO_2RR (eq 3, denoted as H^+-CO_2RR) and, if so, delineating the specific conditions under which it will be operative. This understanding is pivotal for guiding future catalyst design strategies and completing the puzzle surrounding CO_2 reduction.

$$CO_2 + H_2O + 2e^- \rightarrow CO + 2OH^- \quad (1)$$

$$2H_2O + 2e^- \rightarrow H_2 + 2OH^- \quad (2)$$

$$CO_2 + 2H^+ + 2e^- \rightarrow CO + H_2O \quad (3)$$

$$2H^+ + 2e^- \rightarrow H_2 \quad (4)$$

Previous investigations of CO_2RR to CO under neutral and alkaline conditions observed minimal pH dependence,[15−18] suggesting the rate-determining step (RDS) for CO_2-to-CO is highly unlikely to involve proton transfer. Such an effect might relate to the low proton concentration in alkaline/neutral electrolyte; thus, the proton donor is more likely to be the buffer (such as bicarbonate) or water. The reaction pathway could be distinct under acidic conditions due to the abundance of proton.[15] However, the high proton concentration poses challenges in analyzing the current contribution from the CO_2RR and hydrogen evolution reaction (HER) in acid, necessitating an analytical method with high sensitivity.

Herein, we employed a rotating ring-disk electrode (RRDE) with Au (ring)−Au (disk) to investigate the electrode process of CO_2RR in acid, highlighting the direct participation of a proton in the reaction. Surface interrogation scanning electrochemical microscopy (SI-SECM) revealed the prefer-

Received: January 20, 2025
Revised: March 19, 2025
Accepted: March 20, 2025
Published: March 31, 2025

https://doi.org/10.1021/jacs.5c01149
J. Am. Chem. Soc. 2025, 147, 11662−11666

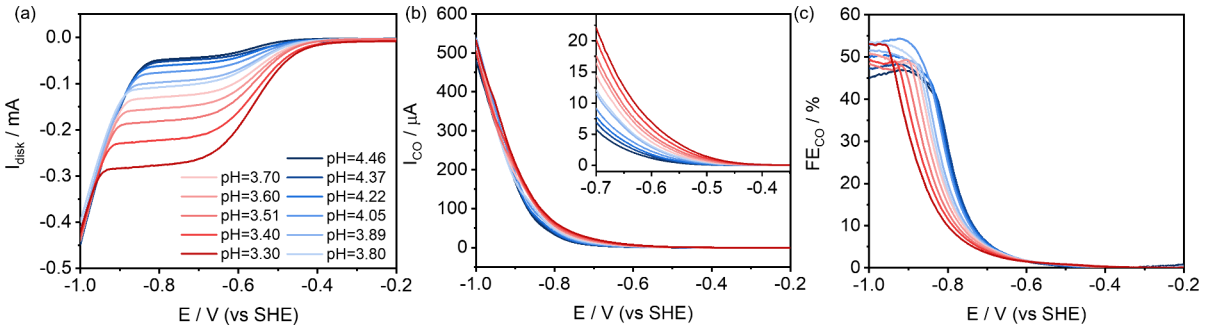

Figure 1. Linear scan voltammogram on Au−Au RRDE in CO_2 saturated 0.1 M $NaClO_4$ under different pHs. The corresponding (a) disk current and (b) CO oxidation on the Au ring. The inset is the zoomed-in low overpotential region. (c) CO FE. Unless otherwise stated, all experimental conditions are controlled at 800 rpm, scan rate = 25 mV/s, and room temperature, and all pH adjustments were achieved by 0.1 M $NaHCO_3$ or concentrated $HClO_4$ to maintain constant Na^+ concentration.

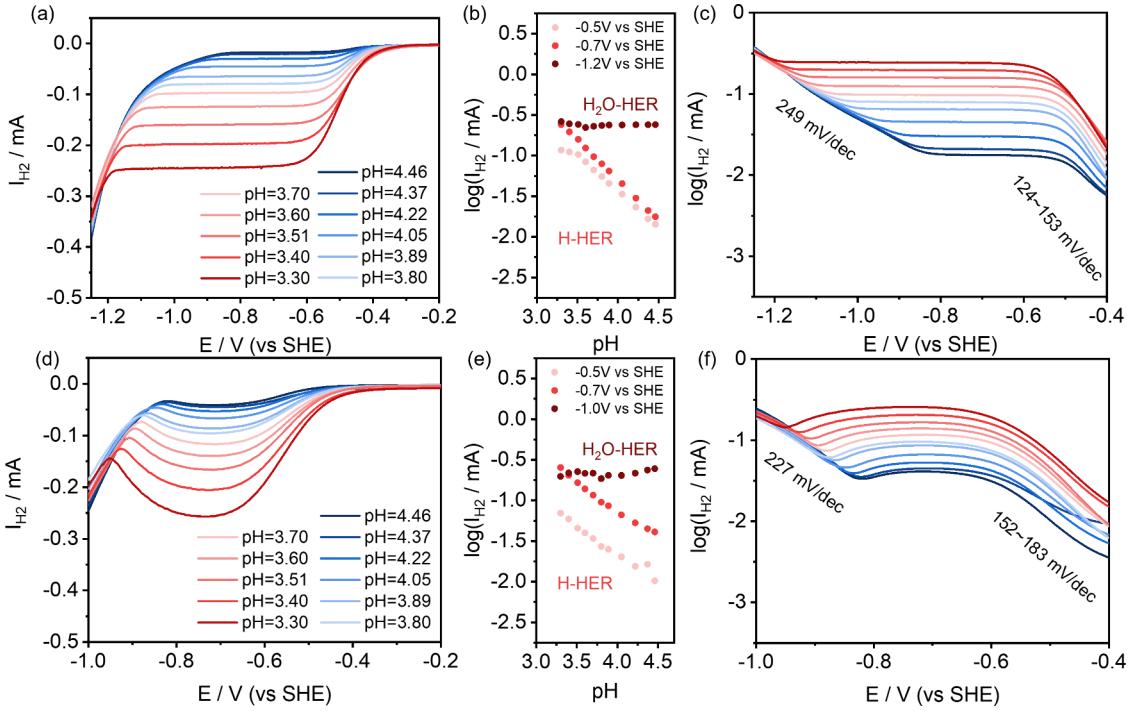

Figure 2. Linear scan voltammograms in Ar (a−c) and CO_2 (d−f) saturated 0.1 M $NaClO_4$ under different pHs. The corresponding HER current (a, d), reaction order in proton at different potentials (b, e), and Tafel plot (c, f).

ential CO_2 adsorption at the low overpotential, outcompeting with the H* to promote the CO_2RR. These findings provide compelling evidence that the CO_2RR with a proton as the direct proton donor should be feasible, offering a promising avenue to address the root cause of the carbonate issue.

The Au−Au RRDE method was employed as reported by Koper et al. (Scheme S2, detailed in Supplementary Method 1).[19−22] The Au disk serves as the working electrode, while the Au ring electrode works as the detector (Figures S1−S5). This configuration ensures efficient in situ detection at the disk electrode, such as pH measurement and product quantification.[19−22] Here, 0.1 M $NaClO_4$ was adopted as the electrolyte with the pH adjusted by 0.1 M $NaHCO_3$ (0.1 M NaOH in the case of Ar conditions) or concentrated $HClO_4$ to ensure constant ionic strength (Table S1), minimizing local Na^+ concentration change during pH adjustment (Figure S6, detailed in Supplementary Note 1).[23−25] Also, the conductivity is sufficiently high that no IR compensation is applied in this study (Figure S7). With these, a high sensitivity of 16 nA/cm^2 (signal-to-noise >10) is achieved, enabling precise investigation at the low overpotential region.

The linear sweep voltammograms (LSVs) on Au−Au RRDE in CO_2 saturated 0.1 M $NaClO_4$ with different bulk pH values are shown in Figure 1. The disk current exhibits a typical mass transport limiting plateau current in the potential region from *ca.* −0.6 V to *ca.* −0.8 V vs SHE (Figures 1a and S8a). The mass transport limiting current and the kinetic current (−0.2 V to *ca.* −0.6 V vs SHE) both showed a clear pH dependence at the SHE scale, indicating the participation of the proton in the reaction (Figure S9). At more negative potential, the current response became pH-insensitive at the SHE scale, similar to previous reports.[20] Benefiting from the high sensitivity of the RRDE, the onset of CO_2RR was confirmed by the increase in the ring current (Figure 1b) and is much earlier than the previous reports.[26−28] Notably, the CO production in this region exhibits a pH-dependent behavior, implying that proton might be involved in the RDS. The Faradaic efficiency (FE) of CO increases with the applied cathodic potential, reaching a

https://doi.org/10.1021/jacs.5c01149
J. Am. Chem. Soc. 2025, 147, 11662−11666

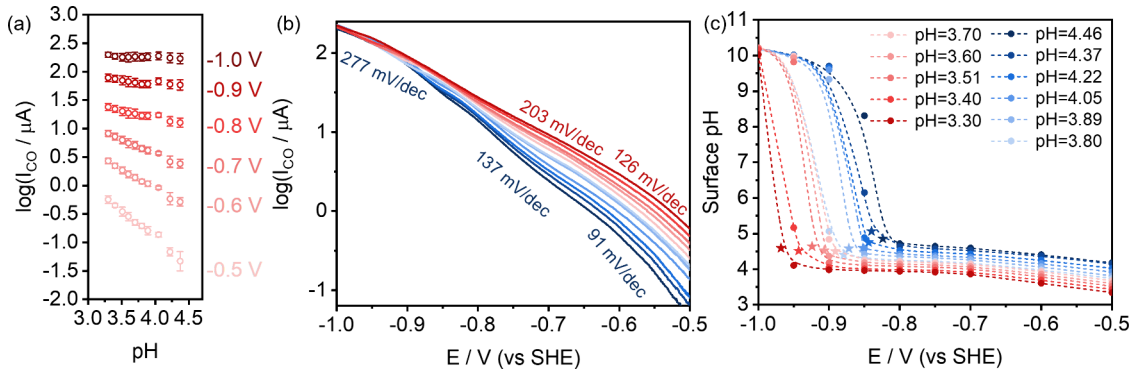

Figure 3. CO_2RR current in CO_2 saturated 0.1 M $NaClO_4$ under different pHs. The corresponding reaction order in proton under different potentials at SHE scale (a), Tafel plot (b), and simulated surface pH (c).

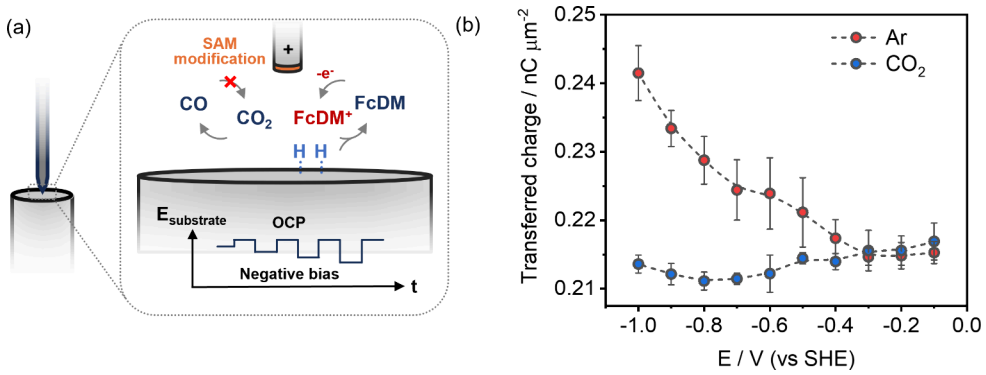

Figure 4. (a) Schematic illustration of SI-SECM in Ar or CO_2 saturated with 0.1 M $NaClO_4$ and 1 mM FcDM electrolyte, pH 3.80. (b) Transferred charge on the probe electrode under different potentials.

peak value of around 50%, further confirming the appreciable contribution from the CO_2RR, even in the pH-dependent region. This finding prompted us to explore the electrode reactions for the acidic CO_2RR in greater depth.

We first examined the behavior of the HER with/without the presence of CO_2 (Figure 2). A nearly first-order proton-dependent relation was observed $\left(\frac{\mathrm{d}\log(j_{\mathrm{H_2},-0.5\mathrm{V}})}{\mathrm{d\,pH}} = -0.90\right)$ before reaching the mass transport limited region under Ar saturated conditions (Figure 2a and 2b), which is similar to that in CO_2 saturated solution (Figure 2e, −0.84). The Tafel slope ranges around 124−153 mV/dec (Figure 2c) indicating the Volmer step ($H^+ + e^- + * \rightarrow H^*$) as the RDS.[29] The Tafel slope in the CO_2 saturated solution is slightly larger than that in the Ar saturated condition (Figure 2f), which will be discussed later. The proton reaction order was 0 at the high overpotential region, regardless of the presence of CO_2. This good agreement with previous reports can be considered as supporting evidence for the hypothesis that a proton is not directly involved in the RDS.[10,12] The Tafel slope in this region is much higher, indicating more sluggish kinetics caused by the additional energy required when water serves as the proton donor (Figure 2c and 2f).[30] We noticed that the LSV of the HER in the presence of CO_2 exhibited a peak-shaped current response (Figure 2d), which is distinct from that observed in the Ar-saturated condition. This behavior implies competition between CO_2RR and HER over reactant and active site which is consistent with the suppressed HER, as indicated by the late onset (Figure S10) and larger Tafel slope (Figure 2c and 2f) in the CO_2-saturated solution.

We further investigated the LSV of the CO_2RR in the different pH electrolytes, as shown in Figure 3. At the low potential region (−0.5 V vs SHE), a first order to the proton concentration for CO_2-to-CO was observed $\left(\frac{\mathrm{d}\log(j_{\mathrm{CO},-0.5\mathrm{V}})}{\mathrm{d\,pH}} = -0.97\right)$ (Figures 1b and 3a). The Tafel slope in this region ranges from 91 to 126 mV/dec, implying the first electron transfer step with a proton as the rate-determining step (Figure 3b). At a potential beyond −0.9 V vs SHE, the reaction order decreased to 0 with an apparent increase in the Tafel slope (Figure 3a,b). This could relate to the elevated surface pH and, thus, a change of the proton donor from proton to water. We then simulated the pH change during LSV in Figure 3c (detailed in Supplementary Method 2, Figure S11). The interfacial pH change is negligible in the pH-dependent region and rapidly rises to alkaline at *ca.* −0.9 V vs SHE, agreeing with the change of the reaction order observed previously. This could explain the decrease in FE_{CO} in Figure 1c, that the highly alkaline condition leads to reduced availability of reactant at the electrode surface.

The discussion presented above provides evidence that H^+-CO_2RR can be realized under acidic conditions. The suppressed HER in the presence of CO_2 prompted us to consider that CO_2 adsorption might happen much earlier so that the H^+-CO_2RR can take place. We then employed SI-SECM to investigate the competitive adsorption of CO_2 and H^+ (Figure 4 and Supplementary Method 3).[31,32] Ferrocene dimethanol (FcDM) is used as a redox mediator, with a Au probe as the detector positioned at 5 μm away from substrate surface (Figure S12 and Scheme S4). The Au probe is

https://doi.org/10.1021/jacs.5c01149
J. Am. Chem. Soc. 2025, 147, 11662−11666

functionalized with a monolayer of $HS(CH_2)_2COOH$ to block the inner sphere electron transfer CO oxidation reaction, while the outer sphere electron transfer of FcDM oxidation remains unaffected (Figure 4a and Figure S13).[33,34] The amount of H* can be selectively titrated by probe-generated $FcDM^+$. As shown in Figure 4b and Figure S14, a continuous increase in the H* coverage is observed in the Ar-saturated solution, while the H* coverage is largely suppressed in the presence of CO_2. The suppressed H* coverage in the presence of CO_2 suggests competitive adsorption between CO_2 and proton, particularly at the low overpotential region. This competitive adsorption could explain the early onset of CO_2RR, as previously observed in the literature.[35−37]

The RDS of acidic CO_2RR is highly likely to be the concerted proton-coupled electron transfer step of the reaction of $CO_2 + H^+ + e^- \rightarrow COOH^*$. At the low overpotential region, proton participation in both the HER and the CO_2RR results in competition for surface active sites and proton, leading to pH dependence on the SHE scale. In contrast, at high overpotential, the elevated local pH shifts the proton donor to water, resulting in a pH-independent behavior similar to neutral and alkaline conditions.[10,15−17] Notably, the pH-dependent regime is of particular interest, as it holds promise for achieving carbonate-free CO_2 electrolysis at the device level. Transitioning to strong acid (pH = 0) can effectively avoid entering the pH-independent region by providing sufficient proton. However, the high proton concentration can significantly influence the apparent reaction rates of both the HER and CO_2RR. To promote H^+-CO_2RR in the presence of high proton concentration, enhancing the intrinsic reaction rate and increasing the local CO_2 concentration is imperative (Table S4).[38] Given the difference in intrinsic kinetics between the CO_2RR and HER on the existing catalyst (Table S5), manipulating other factors to alter the apparent reaction rate may prove beneficial. The intermediate dipole moment of HER and H^+-CO_2RR exhibits diverse responses to the electrode potential and interfacial electrical field.[39] Thus, modulating the interfacial electrical field to stabilize intermediates and enhance the local CO_2 concentration could effectively promote the apparent reaction rate of H^+-CO_2RR. This rationale underlies the enhanced activity reported for CO_2RR in strong acid through the utilization of high cation concentration and ionomer-modified electrodes.[7,40−42]

In conclusion, we demonstrated that the CO_2RR can utilize a proton as a reactant under locally acidic conditions using a high-sensitivity Au−Au RRDE. SI-SECM suggests preferential CO_2 adsorption at lower overpotential, suppressing the competitive H* adsorption to promote the CO_2RR in acid. These findings reveal the fundamental mechanism underpinning proton-coupled CO_2 reduction in acidic media and indicate that carbonate-free CO_2 electrolysis could be viable. Since the intrinsic kinetics of proton-coupled CO_2 reduction is comparable to HER on Au, identifying catalysts with superior intrinsic activity or modulating the reaction thermodynamics is required.

■ ASSOCIATED CONTENT

Supporting Information

The Supporting Information is available free of charge at https://pubs.acs.org/doi/10.1021/jacs.5c01149.

More details in experimental procedure, simulation methods, and electrochemical data (PDF)

■ AUTHOR INFORMATION

Corresponding Author

Ying Wang − *Department of Chemistry, The Chinese University of Hong Kong, New Territories, Hong Kong S. A. R., China;* orcid.org/0000-0002-6240-5535; Email: ying.b.wang@cuhk.edu.hk

Author

Weixing Wu − *Department of Chemistry, The Chinese University of Hong Kong, New Territories, Hong Kong S. A. R., China*

Complete contact information is available at: https://pubs.acs.org/10.1021/jacs.5c01149

Notes

The authors declare no competing financial interest.

■ ACKNOWLEDGMENTS

Y.W. and W.W. acknowledge the financial support from the Excellent Young Scientist Fund (Hongkong and Macau) from the National Natural Science Foundation of China (project no. 22222208) and the Research Grants Council of the Hong Kong Special Administrative Region (project no. 14305323). The authors acknowledge the Department of Mechanical and Automation Engineering, The Chinese University of Hong Kong for the support of COMSOL.

■ REFERENCES

(1) Stephens, I. E. L.; Chan, K.; Bagger, A.; Boettcher, S. W.; Bonin, J.; Boutin, E.; Buckley, A. K.; Buonsanti, R.; Cave, E. R.; Chang, X.; Chee, S. W.; da Silva, A. H. M.; de Luna, P.; Einsle, O.; Endrődi, B.; Escudero-Escribano, M.; Ferreira de Araujo, J. V.; Figueiredo, M. C.; Hahn, C.; Hansen, K. U.; Haussener, S.; Hunegnaw, S.; Huo, Z.; Hwang, Y. J.; Janáky, C.; Jayathilake, B. S.; Jiao, F.; Jovanov, Z. P.; Karimi, P.; Koper, M. T. M.; Kuhl, K. P.; Lee, W. H.; Liang, Z.; Liu, X.; Ma, S.; Ma, M.; Oh, H.-S.; Robert, M.; Cuenya, B. R.; Rossmeisl, J.; Roy, C.; Ryan, M. P.; Sargent, E. H.; Sebastián-Pascual, P.; Seger, B.; Steier, L.; Strasser, P.; Varela, A. S.; Vos, R. E.; Wang, X.; Xu, B.; Yadegari, H.; Zhou, Y. 2022 roadmap on low temperature electrochemical CO2 reduction. *J. Phys. Energy* **2022**, *4* (4), No. 042003.

(2) Masel, R. I.; Liu, Z.; Yang, H.; Kaczur, J. J.; Carrillo, D.; Ren, S.; Salvatore, D.; Berlinguette, C. P. An industrial perspective on catalysts for low-temperature CO2 electrolysis. *Nat. Nanotechnol.* **2021**, *16* (2), 118−128.

(3) Grim, R. G.; Ferrell Iii, J. R.; Huang, Z.; Tao, L.; Resch, M. G. The feasibility of direct CO2 conversion technologies on impacting mid-century climate goals. *Joule* **2023**, *7* (8), 1684−1699.

(4) Sun, J. W.; Fu, H. Q.; Liu, P. F.; Chen, A.; Liu, P.; Yang, H. G.; Zhao, H. Advances and challenges in scalable carbon dioxide electrolysis. *EES Catal.* **2023**, *1* (6), 934−949.

(5) Chen, Q.; Wang, X.; Zhou, Y.; Tan, Y.; Li, H.; Fu, J.; Liu, M. Electrocatalytic CO2 Reduction to C2+ Products in Flow Cells. *Adv. Mater.* **2024**, *36* (5), No. 2303902.

(6) Wu, W.; Xu, L.; Lu, Q.; Sun, J.; Xu, Z.; Song, C.; Yu, J. C.; Wang, Y. Addressing the Carbonate Issue: Electrocatalysts for Acidic CO2 Reduction Reaction. *Adv. Mater.* **2025**, *37*, No. 2312894.

(7) Pan, B.; Fan, J.; Zhang, J.; Luo, Y.; Shen, C.; Wang, C.; Wang, Y.; Li, Y. Close to 90% Single-Pass Conversion Efficiency for CO2 Electroreduction in an Acid-Fed Membrane Electrode Assembly. *ACS Energy Lett.* **2022**, *7* (12), 4224−4231.

(8) O'Brien, C. P.; Miao, R. K.; Liu, S.; Xu, Y.; Lee, G.; Robb, A.; Huang, J. E.; Xie, K.; Bertens, K.; Gabardo, C. M.; Edwards, J. P.; Dinh, C.-T.; Sargent, E. H.; Sinton, D. Single Pass CO2 Conversion Exceeding 85% in the Electrosynthesis of Multicarbon Products via Local CO2 Regeneration. *ACS Energy Lett.* **2021**, *6* (8), 2952−2959.
(9) Xu, Z.; Xie, Y.; Wang, Y. Pause electrolysis for acidic CO2 reduction on 3-dimensional Cu. *MRE* **2023**, *3* (1), No. 100173.
(10) Zhang, Z.; Lu, Q.; Sun, J.; Li, G.; Wu, W.; Xu, Z.; Xu, L.; Wang, Y. Unravelling the carbonate issue through the regulation of mass transport and charge transfer in mild acid. *Chem. Sci.* **2024**, *15* (8), 2786−2791.
(11) Wang, Z.; Li, Y.; Zhao, X.; Chen, S.; Nian, Q.; Luo, X.; Fan, J.; Ruan, D.; Xiong, B.-Q.; Ren, X. Localized Alkaline Environment via In Situ Electrostatic Confinement for Enhanced CO2-to-Ethylene Conversion in Neutral Medium. *J. Am. Chem. Soc.* **2023**, *145* (11), 6339−6348.
(12) Bondue, C. J.; Graf, M.; Goyal, A.; Koper, M. T. M. Suppression of Hydrogen Evolution in Acidic Electrolytes by Electrochemical CO2 Reduction. *J. Am. Chem. Soc.* **2021**, *143* (1), 279−285.
(13) Ooka, H.; Figueiredo, M. C.; Koper, M. T. M. Competition between Hydrogen Evolution and Carbon Dioxide Reduction on Copper Electrodes in Mildly Acidic Media. *Langmuir* **2017**, *33* (37), 9307−9313.
(14) Wu, W.; Lu, Q.; Li, G.; Wang, Y. How to extract kinetic information from Tafel analysis in electrocatalysis. *J. Chem. Phys.* **2023**, *159* (22), No. 221501.
(15) Ringe, S.; Morales-Guio, C. G.; Chen, L. D.; Fields, M.; Jaramillo, T. F.; Hahn, C.; Chan, K. Double layer charging driven carbon dioxide adsorption limits the rate of electrochemical carbon dioxide reduction on Gold. *Nat. Commun.* **2020**, *11* (1), 33.
(16) Wuttig, A.; Yoon, Y.; Ryu, J.; Surendranath, Y. Bicarbonate Is Not a General Acid in Au-Catalyzed CO2 Electroreduction. *J. Am. Chem. Soc.* **2017**, *139* (47), 17109−17113.
(17) Deng, W.; Zhang, P.; Seger, B.; Gong, J. Unraveling the rate-limiting step of two-electron transfer electrochemical reduction of carbon dioxide. *Nat. Commun.* **2022**, *13* (1), 803.
(18) Marcandalli, G.; Goyal, A.; Koper, M. T. M. Electrolyte Effects on the Faradaic Efficiency of CO2 Reduction to CO on a Gold Electrode. *ACS Catal.* **2021**, *11* (9), 4936−4945.
(19) Goyal, A.; Marcandalli, G.; Mints, V. A.; Koper, M. T. M. Competition between CO2 Reduction and Hydrogen Evolution on a Gold Electrode under Well-Defined Mass Transport Conditions. *J. Am. Chem. Soc.* **2020**, *142* (9), 4154−4161.
(20) Liu, X.; Koper, M. T. M. Tuning the Interfacial Reaction Environment for CO2 Electroreduction to CO in Mildly Acidic Media. *J. Am. Chem. Soc.* **2024**, *146* (8), 5242−5251.
(21) Zhang, F.; Co, A. C. Direct Evidence of Local pH Change and the Role of Alkali Cation during CO2 Electroreduction in Aqueous Media. *Angew. Chem., Int. Ed.* **2020**, *59* (4), 1674−1681.
(22) Cui, Z.; Wong, A. J.-W.; Janik, M. J.; Co, A. C. Negative Reaction Order for CO during CO2 Electroreduction on Au. *J. Am. Chem. Soc.* **2024**, *146* (34), 23872−23880.
(23) Monteiro, M. C. O.; Dattila, F.; López, N.; Koper, M. T. M. The Role of Cation Acidity on the Competition between Hydrogen Evolution and CO2 Reduction on Gold Electrodes. *J. Am. Chem. Soc.* **2022**, *144* (4), 1589−1602.
(24) Monteiro, M. C. O.; Dattila, F.; Hagedoorn, B.; García-Muelas, R.; López, N.; Koper, M. T. M. Absence of CO2 electroreduction on copper, gold and silver electrodes without metal cations in solution. *Nat. Catal.* **2021**, *4* (8), 654−662.
(25) Marcandalli, G.; Monteiro, M. C. O.; Goyal, A.; Koper, M. T. M. Electrolyte Effects on CO2 Electrochemical Reduction to CO. *Acc. Chem. Res.* **2022**, *55* (14), 1900−1911.
(26) Deng, W.; Zhang, P.; Seger, B.; Gong, J. Unraveling the rate-limiting step of two-electron transfer electrochemical reduction of carbon dioxide. *Nat. Commun.* **2022**, *13* (1), 803.
(27) Wuttig, A.; Yaguchi, M.; Motobayashi, K.; Osawa, M.; Surendranath, Y. Inhibited proton transfer enhances Au-catalyzed CO2-to-fuels selectivity. *Proc. Natl. Acad. Sci. U. S. A.* **2016**, *113* (32), E4585−E4593.
(28) Dunwell, M.; Luc, W.; Yan, Y.; Jiao, F.; Xu, B. Understanding Surface-Mediated Electrochemical Reactions: CO2 Reduction and Beyond. *ACS Catal.* **2018**, *8* (9), 8121−8129.
(29) Shinagawa, T.; Garcia-Esparza, A. T.; Takanabe, K. Insight on Tafel slopes from a microkinetic analysis of aqueous electrocatalysis for energy conversion. *Sci. Rep.* **2015**, *5* (1), 13801.
(30) Zhu, S.; Liu, X.; Wang, X.; Zhao, Q.; Shao, M. Some remaining puzzles in hydrogen electrocatalysis mechanisms on platinum surfaces. *Joule* **2024**, *8* (7), 1890−1918.
(31) Jin, Z.; Li, P.; Fang, Z.; Yu, G. Emerging Electrochemical Techniques for Probing Site Behavior in Single-Atom Electrocatalysts. *Acc. Chem. Res.* **2022**, *55* (5), 759−769.
(32) Ahn, H. S.; Bard, A. J. Electrochemical Surface Interrogation of a MoS2 Hydrogen-Evolving Catalyst: In Situ Determination of the Surface Hydride Coverage and the Hydrogen Evolution Kinetics. *J. Phys. Chem. Lett.* **2016**, *7* (14), 2748−2752.
(33) Bard, A. J. Inner-Sphere Heterogeneous Electrode Reactions. Electrocatalysis and Photocatalysis: The Challenge. *J. Am. Chem. Soc.* **2010**, *132* (22), 7559−7567.
(34) Xiao, X.; Pan, S.; Jang, J. S.; Fan, F.-R. F.; Bard, A. J. Single Nanoparticle Electrocatalysis: Effect of Monolayers on Particle and Electrode on Electron Transfer. *J. Phys. Chem. C* **2009**, *113* (33), 14978−14982.
(35) Xie, Y.; Ou, P.; Wang, X.; Xu, Z.; Li, Y. C.; Wang, Z.; Huang, J. E.; Wicks, J.; McCallum, C.; Wang, N.; Wang, Y.; Chen, T.; Lo, B. T. W.; Sinton, D.; Yu, J. C.; Wang, Y.; Sargent, E. H. High carbon utilization in CO2 reduction to multi-carbon products in acidic media. *Nat. Catal.* **2022**, *5* (6), 564−570.
(36) Yu, X.; Xu, Y.; Li, L.; Zhang, M.; Qin, W.; Che, F.; Zhong, M. Coverage enhancement accelerates acidic CO2 electrolysis at ampere-level current with high energy and carbon efficiencies. *Nat. Commun.* **2024**, *15* (1), 1711.
(37) Sun, B.; Li, Z.; Xiao, D.; Liu, H.; Song, K.; Wang, Z.; Liu, Y.; Zheng, Z.; Wang, P.; Dai, Y.; Huang, B.; Thomas, A.; Cheng, H. Unveiling pH-Dependent Adsorption Strength of *CO2− Intermediate over High-Density Sn Single Atom Catalyst for Acidic CO2-to-HCOOH Electroreduction. *Angew. Chem., Int. Ed.* **2024**, *63* (14), No. e202318874.
(38) Kastlunger, G.; Wang, L.; Govindarajan, N.; Heenen, H. H.; Ringe, S.; Jaramillo, T.; Hahn, C.; Chan, K. Using pH Dependence to Understand Mechanisms in Electrochemical CO Reduction. *ACS Catal.* **2022**, *12* (8), 4344−4357.
(39) Vijay, S.; Ju, W.; Brückner, S.; Tsang, S.-C.; Strasser, P.; Chan, K. Unified mechanistic understanding of CO2 reduction to CO on transition metal and single atom catalysts. *Nat. Catal.* **2021**, *4* (12), 1024−1031.
(40) Huang, J. E.; Li, F.; Ozden, A.; Sedighian Rasouli, A.; García de Arquer, F. P.; Liu, S.; Zhang, S.; Luo, M.; Wang, X.; Lum, Y.; Xu, Y.; Bertens, K.; Miao, R. K.; Dinh, C.-T.; Sinton, D.; Sargent, E. H. CO2 electrolysis to multicarbon products in strong acid. *Science* **2021**, *372* (6546), 1074−1078.
(41) Gu, J.; Liu, S.; Ni, W.; Ren, W.; Haussener, S.; Hu, X. Modulating electric field distribution by alkali cations for CO2 electroreduction in strongly acidic medium. *Nat. Catal.* **2022**, *5* (4), 268−276.
(42) Zhao, Y.; Hao, L.; Ozden, A.; Liu, S.; Miao, R. K.; Ou, P.; Alkayyali, T.; Zhang, S.; Ning, J.; Liang, Y.; Xu, Y.; Fan, M.; Chen, Y.; Huang, J. E.; Xie, K.; Zhang, J.; O'Brien, C. P.; Li, F.; Sargent, E. H.; Sinton, D. Conversion of CO2 to multicarbon products in strong acid by controlling the catalyst microenvironment. *Nat. Synth.* **2023**, *2* (5), 403−412.

https://doi.org/10.1021/jacs.5c01149
J. Am. Chem. Soc. 2025, 147, 11662−11666